Interpreting the temperature of water at cold springs and the importance of gravitational potential energy

Michael Manga and James W. Kirchner

Department of Earth and Planetary Science, University of California, Berkeley, Berkeley, California, USA

Received 25 November 2003; revised 22 March 2004; accepted 31 March 2004; published 19 May 2004.

[1] Circulating groundwater transports heat. If groundwater flow velocities are sufficiently high, most of the subsurface heat transport can occur by advection. This is the case, for example, in the Cascades volcanic arc where much of the background geothermal heat is transported advectively and then discharged when the groundwater emerges at springs. The temperature of spring water can thus be used to infer the geothermal heat flux. If spring water temperature is many degrees warmer than the ambient temperature, as it is at hot springs, determining the heat discharged at springs is straightforward. At large-volume cold springs, however, the geothermal warming of water is small because the added heat is diluted in a large volume of water. We show that in order to interpret the temperature of cold springs we must account for three processes: (1) conversion of gravitational potential energy to heat through viscous dissipation, (2) conduction of heat to or from the Earth's surface, and (3) geothermal warming. Using spring temperature data from the central Oregon Cascades and Mount Shasta, California, we show that the warming due to surface heat exchange and dissipation of gravitational potential energy can be comparable to that due to geothermal heating. Unless these confounding sources of heating are taken into account, estimates of geothermal heat flux derived from temperatures of cold springs can be incorrect by large factors. *INDEX TERMS:* 1829 Hydrology: Groundwater hydrology; 8130 Tectonophysics: Heat generation and transport; 8424 Volcanology: Hydrothermal systems (8135); *KEYWORDS:* geothermal heat, gravitational potential energy, spring

Citation: Manga, M., and J. W. Kirchner (2004), Interpreting the temperature of water at cold springs and the importance of gravitational potential energy, *Water Resour. Res.*, *40*, W05110, doi:10.1029/2003WR002905.

1. Introduction

[2] Water moving through a groundwater system transports heat and thus changes the subsurface temperature distribution. Temperature can therefore be used as a tracer of hydrologic processes and for testing conceptual hydrogeologic models [e.g., *Andrews et al.*, 1982]. Temperature offers several advantages as a tracer because it is easy, quick, and inexpensive to measure accurately in the field. The temperature of groundwater also provides insight into the subsurface geological processes that generate heat.

[3] Several previous studies have developed models for predicting or interpreting spring temperatures. These include analytical models to interpret seasonal temperature fluctuations [e.g., *Bundschuh*, 1993] and numerical models to study regional-scale flows [e.g., *Forster and Smith*, 1989]. The general conclusion of these models is that the predicted temperature of spring water depends on the volume flux of water. For a given aquifer, as the groundwater velocity increases, the heat added by geothermal warming is diluted into larger volumes of water, and consequently, spring temperatures become colder. In fact, spring temperatures can be colder than the mean annual surface temperature at the discharge elevation if the water is recharged at much higher elevations, as first noted by Alexander von Humboldt in 1844 [*Davis*, 1999]. In contrast, for very low velocities (typically a result of low permeabilities), the subsurface temperature gradient is nearly undisturbed by groundwater flow and the temperature of spring water will be close to the mean annual surface temperature at the discharge elevation. The warmest spring temperatures occur for an intermediate range of velocities such that groundwater flow removes most of the geothermal heat flux advectively, but the added heat is not diluted by large volumes of water [*Forster and Smith*, 1989]. In this latter case, the temperature of spring water can be used to infer the background geothermal heat flux provided the area from which heat is collected is known [e.g., *Ingebritsen et al.*, 1989].

[4] In this paper we develop an analytical model that includes a contribution to the thermal budget of spring water that is usually neglected (see *Domenico* [1972, p. 160] for a calculation in which it is included): the conversion of gravitational potential energy (hereinafter referred to as GPE) to heat. We then apply this model to cold springs in the Oregon and California Cascades. For these springs we show that the change in elevation and discharge are sufficiently large that the dissipation of gravitational potential energy sometimes dominates the inferred warming of discharged spring water. We argue that ignoring GPE can lead to significant errors in the amount of geothermal warming of water discharged at cold springs.

2. Local Energy Balance

[5] Consider the steady flow of water through the aquifer shown in Figure 1. The thermal energy balance for a parcel

0043-1397/04/2003WR002905$09.00

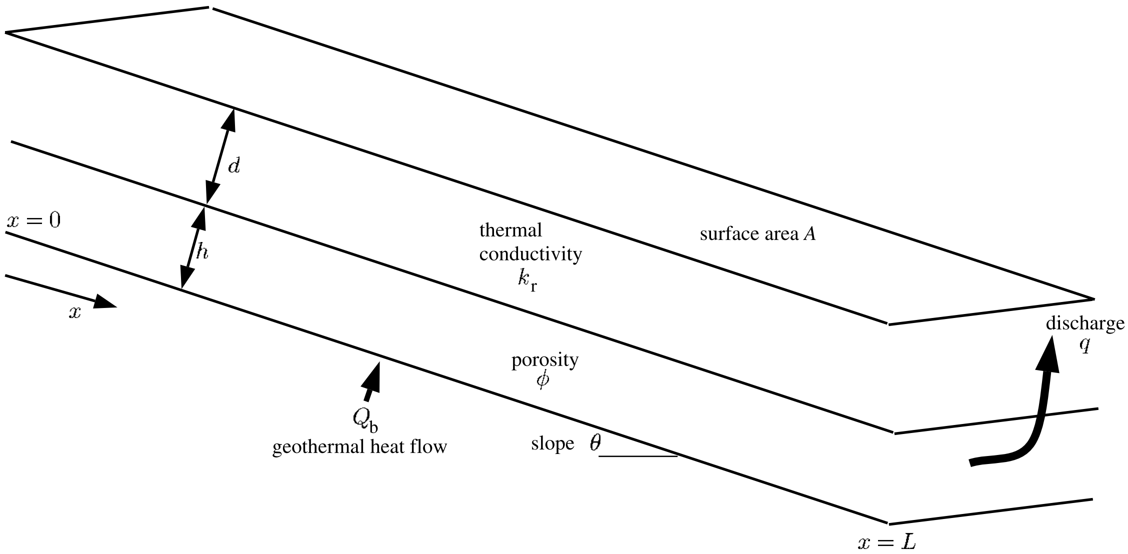

Figure 1. Geometry of model problem. Aquifer length is L, its thickness is h, and it is located at depth d below the surface.

of water with height h and moving with pore velocity u and Darcy velocity $u\phi$, where ϕ is the porosity, is given by

$$\underbrace{\rho_w \phi h C_w \frac{dT}{dt}}_{\text{rate of change of thermal energy}} = \underbrace{\rho_w g h \phi u \sin\theta}_{\text{gravitational potential energy (GPE) dissipation}} + \underbrace{\frac{k_r (T_s - T)}{d}}_{\text{heat transfer to/from surface}} + \underbrace{Q_b}_{\text{geothermalwarming}} . \quad (1)$$

Here subscripts w and r indicate properties of water and saturated rock, respectively, k is thermal conductivity, ρ is density, C is specific heat, g is gravitational acceleration, Q_b is the background geothermal heat flux, and d and θ are the depth and slope of the water table. T and T_s are the temperatures at the water table and Earth's surface, respectively. Whereas the first and third terms on the right-hand side of equation (1) are positive, the second term is typically negative. Notice that fluid properties such as viscosity, and geometric properties of the porous material such as tortuosity and permeability, do not enter into equation (1) explicitly; these properties, however, influence u.

3. Predicted Temperature of Spring Water

[6] In order to determine the relative contribution of the three heat sources/sinks (the three terms on the right-hand side of equation (1)) to the temperature of spring water, we need to apply equation (1) to an aquifer. Consider a model for an aquifer in which water enters one end (x = 0) at temperature T_0 and is discharged at the other end ($x = L$) at a temperature $T_0 + \Delta T$. The water flows through the aquifer in the x direction, and we assume that at any given position x, the temperature of the aquifer is uniform across its thickness; that is, it is thermally well mixed [*Langseth and Herman*, 1981]. The well-mixed aquifer model is a good approximation in situations where advective heat transfer is important [*Fisher and Becker*, 2000; *Rosenberg et al.*, 2000]. To determine ΔT, we can integrate equation (1) along the length of the aquifer by replacing dT/dt with $u(x)dT/dx$, where u is the pore velocity.

[7] The mean residence time of water in the aquifer is L/u. From conservation of mass, the mean residence time is also $\phi h\, A/q = \phi h/R$, where q is the spring discharge, A is the area of the aquifer (see Figure 1), and R is the mean recharge rate. The mean pore velocity u can thus be replaced by $qL/\phi h\, A$.

[8] The temperature boundary condition at the land surface varies with elevation,

$$T_s(x) = T_0 - x \sin\theta \frac{dT_s}{dz}, \quad (2)$$

where T_0 is the surface temperature at x = 0 and dT_s/dz is the adiabatic lapse rate. We will assume for now that at x = 0, $T = T_0$; that is, the recharge temperature is the same as the surface temperature at the recharge elevation.

[9] Integrating equation (1) with equation (2) as a surface boundary condition yields

$$\Delta T = \left(\frac{Q_b d}{\rho_w C_w \kappa_r} + \frac{g\Delta z}{\beta C_w}\right)\left(e^{\beta} - 1\right) - \frac{\Delta z}{\beta}\left(1 + \beta - e^{\beta}\right)\frac{dT_s}{dz}, \quad (3)$$

where $\beta = \kappa_r A/dq$, $\kappa_r = k_r/\rho_w C_w$, and Δz is the change in elevation between the recharge and discharge elevations.

[10] In the limit that conductive heat transfer to and from the surface can be ignored (equivalent to the limit $dq/A\kappa_r \to \infty$), equation (3) simplifies to

$$\Delta T = \underbrace{\frac{Q_b A}{\rho_w C_w q}}_{\text{geothermal warming}} + \underbrace{\frac{\Delta z g}{C_w}}_{\text{GPE dissipation}} . \quad (4)$$

We will characterize the relative importance of geothermal and GPE warming by

$$\Lambda = \frac{\text{geothermal warming}}{\text{GPE dissipation}} = \frac{Q_b A}{\rho g q \Delta z}. \quad (5)$$

A version of equation (4) that ignores the contribution of GPE warming has been applied in previous studies to estimate Q_b from measurements of ΔT [e.g., *Brott et al.*, 1981; *Ingebritsen et al.*, 1989; *Manga*, 1998] or to infer the recharge area A [e.g., *van der Kamp and Bachu*, 1989]. As we show next, however, in some cases the contribution of GPE warming can be sufficiently large to influence the inferred Q_b.

4. Is the Conversion of Gravitational Potential Energy Significant?

[11] Evaluating the gravitational potential energy term in equation (4), we expect a temperature increase of $dT/dz = g/C_w \approx 2.3$°C/km. This is a small gradient compared with a typical geothermal gradient, 20–100°C/km [e.g., *Pollack et al.*, 1993], and less than the wet adiabatic lapse rate of about 5°C/km. Nevertheless, it is large enough to matter in situations where there are large volumes of flowing groundwater (high recharge rates) and large elevation changes of the order of 1 km. These are both conditions that characterize large-volume springs on volcanoes, for example.

[12] Figure 2a shows the predicted change in temperature ΔT for the model problem. For purposes of generality, all quantities other than ΔT are made dimensionless. The dashed curve neglects GPE and geothermal warming. The solid curves include GPE warming. In Figure 2, Λ is the ratio of geothermal warming and GPE dissipation defined by equation (5).

[13] Figure 2b shows ΔT as a function of aquifer depth d. In Figure 2b, model parameters are typical of those for the springs in the Oregon and California Cascades. The temperature at the recharge elevation is assumed to be 0.5°C, and the surface temperature at the discharge elevation, 1 km lower, is 6°C. The geothermal heat flux Q_b is 100 mW/m^2. In Figure 2b, discharge q is assumed to be equivalent to three different recharge rates ($R = q/A$): 0.1, 0.5, and 2 m/yr. $R = 0.5$ m/yr is typical in the Cascades [*Ingebritsen et al.*, 1994; *Manga*, 1997].

[14] Figure 2 shows three important features of the model problem. First, if the aquifers are close to the surface (d less than a few meters), springs will discharge water at temperatures close to the mean annual surface temperature. This is because the timescale for water to flow through the aquifer is long compared with the thermal diffusion timescale, so that water in the aquifer is able to equilibrate with the surface temperature. Second, dissipation of gravitational potential energy results in temperature increases of about 2°C for aquifers deep enough that heat transfer to the surface is negligible (compare the dashed curve in Figure 2a with the solid curve with $\Lambda = 0$ for large d). Third, as illustrated in Figure 2b, sufficiently low recharge rates and large depths (equivalent to large Λ and small β) are needed for spring temperatures to exceed the temperature at the discharge location; for high velocities, water temperature will be colder than the temperature at the discharge elevation even if the background heat flux is high, as it is in this example. A more general conclusion is that when spring temperatures are cold and discharge is high, all three processes considered here (geothermal heating, GPE dissipation, and heat transfer to the surface) may need to be considered to interpret spring temperatures.

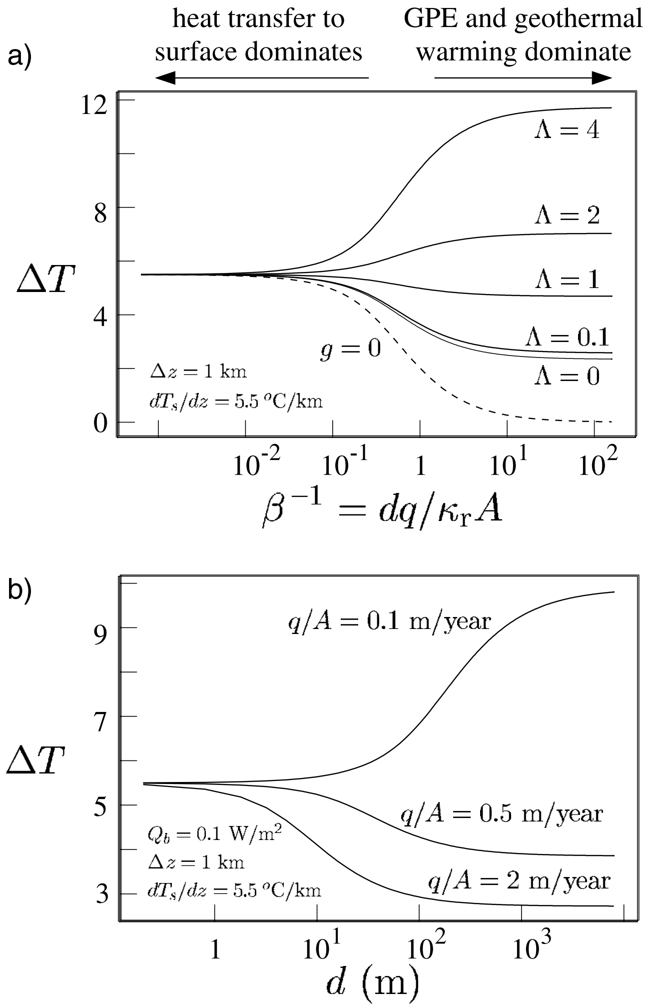

Figure 2. (a) Relationship between ΔT and dimensionless aquifer depth, as described by equation (3). The dashed curve ignores the contribution to warming provided by gravitational potential energy (GPE) dissipation. Λ, defined in equation (5), is the ratio of geothermal warming to GPE dissipation. (b) Relationship between temperature change and water table depth when the equivalent mean recharge is 0.1, 0.5, and 2 m/yr. The background heat flux is 100 mW/m^2. The change in elevation Δz between recharge and discharge elevation is 1 km.

[15] An example of a large-volume cold "spring" is the set of springs discharging into the Fall River at the base of Medicine Lake Volcano, California. These springs discharge about 40 m^3/s [*Meinzer*, 1927]. The recharge area is an approximately 2000-km^2 region on the flanks of the Medicine Lake shield volcano. While recharge is distributed over a broad area, we will assume for simplicity that the model shown in Figure 1 is still a reasonable approximation. A highly simplified sketch of the geometry of the system is shown in Figure 3.

[16] Assuming a mean recharge of 0.5 m/yr [*Rose et al.*, 1996] and that the depth of the aquifer is greater than 100 m, Figure 2 implies that the change in temperature is dominated by geothermal warming and GPE dissipation. In fact, if conductive heat transfer to and from the

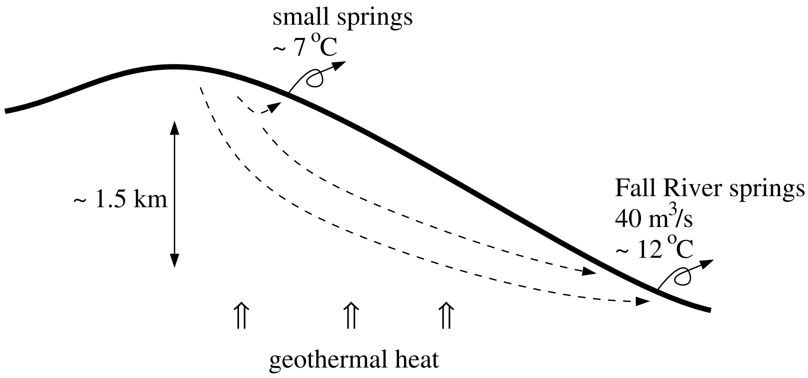

Figure 3. Schematic illustration of the the groundwater system at Medicine Lake Volcano, California. Typical temperatures of small, high-elevation springs are 7°C, whereas a typical large spring discharging into the Fall River is 12°C [*Rose et al.*, 1996]. The increase in water temperature between the recharge discharge elevation is about 5°C, of which about 3°C can be attributed to GPE warming. The mean discharge of the springs is about 40 m^3/s. Hence the total heat discharge is about 360 MW. The spatial area of the aquifer or groundwater system that delivers water to the Fall River springs is about 2000 km^2; assuming all the background heat flux is removed advectively by groundwater and discharged at the Fall River springs, the mean geothermal flux is about 0.16 W/m^2.

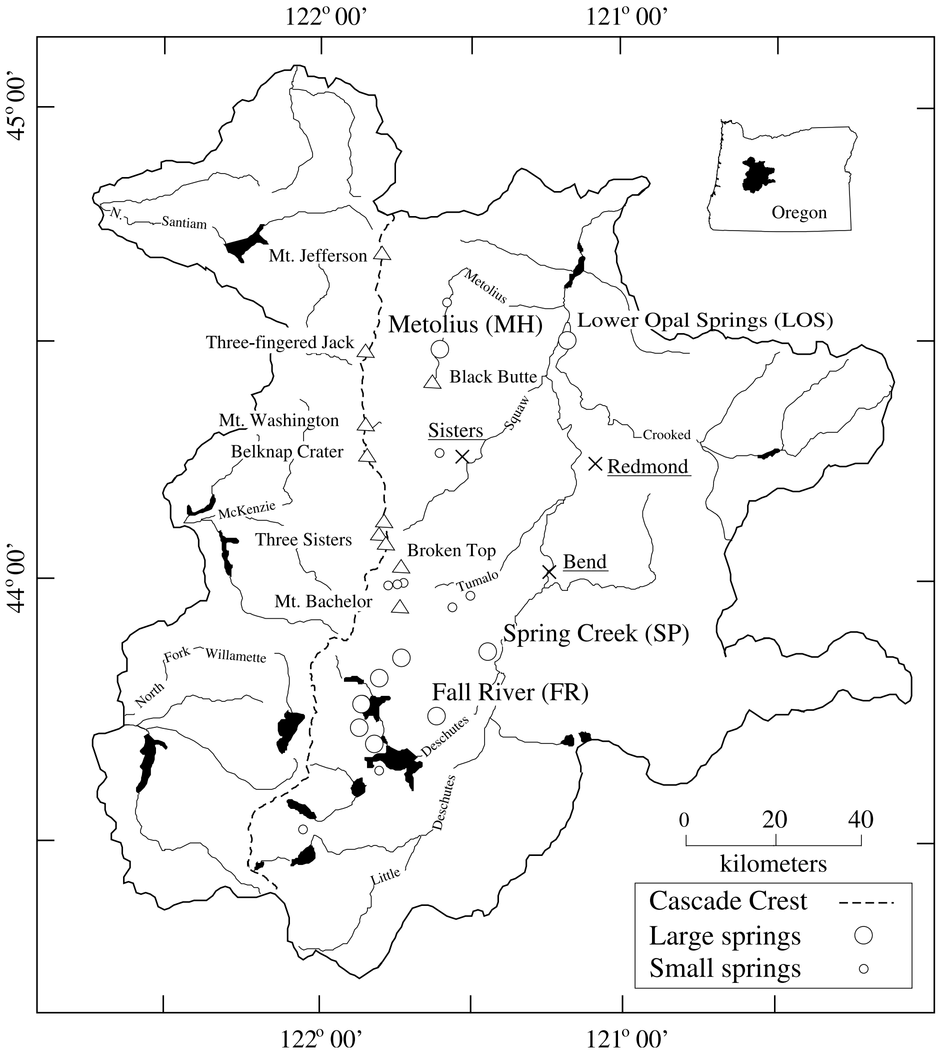

Figure 4. Map of the central Oregon Cascades, showing the location of large springs (discharge >0.5 m^3/s), small springs, rivers, the peaks of large strato and shield volcanoes, and towns.

Table 1. Springs at Mount Shasta and Central Oregon Cascades[a]

Name	Elevation, m	Temperature, °C	$\delta^{18}O$, permil	Recharge Elevation,[b] m	Temperature Corrected for GPE,[c] °C
			Mount Shasta		
Beaughton Creek	1146	7.0	−14.6	2771	3.3
Big	1097	6.8	−14.5	2721	3.1
Big Canyon	1512	4.4	−13.8	2371	2.4
Black Butte	1204	7.6	−14.1	2521	4.6
East Squaw	933	7.1	−13.0	1971	4.7
Green Butte	2621	1.7	−14.3	2621	1.7
Heron	878	7.2	−13.4	2171	4.2
Intake	1402	5.4	−13.1	2021	4.0
McCloud	939	6.8	−13.0	1971	4.4
McGinnis	1768	4.5	−13.3	2121	3.7
North Ash	2057	2.6	−14.3	2621	1.3
Panther Meadow	2353	2.9	−14.1	2521	2.5
South Brewer	2045	2.5	−14.2	2571	1.3
Squaw Meadow	2499	1.7	−14.0	2471	1.7
Widow	1408	3.9	−12.8	1871	2.8
			Central Oregon Cascades		
Big	1317	4.3	−15.1	2335	2.0
Black Pine	1320	4.8	−14.7	2113	3.0
Browns	1332	3.8	−14.0	1724	2.9
Cold	1036	5.0	−13.3	1335	4.3
Cultus	1356	3.4	−14.1	1779	2.4
Fall	1286	6.1	−14.1	1779	5.1
Lower Opal	597	12.0	−15.3	2446	7.8
Melvin	1329	4.8	−14.7	2113	3.0
Metolius	920	8.2	−14.6	2168	5.3
North Davis	1323	3.4	−14.1	1779	2.4
Quinn	1354	3.4	−13.7	1556	2.9
Snow Creek	1378	5.4	−14.1	1779	4.5
Spring River	1268	8.0	−14.6	2168	5.9
Unnamed	1329	3.5	−13.9	1668	2.7
Unnamed	1682	3.3	−13.8	1612	3.3
Unnamed	829	5.3	−13.6	1501	3.7
Unnamed	1658	1.7	−13.8	1612	1.7
Unnamed	1658	3.6	−13.9	1668	3.6

[a]Mount Shasta data are from *Nathenson et al.* [2003], and Central Oregon Cascades data are from *James* [1999]. Bold type indicates large-volume cold springs.

[b]Mount Shasta: Assuming the $\delta^{18}O$ value of Green Butte represents recharge at that elevation and that $\delta^{18}O$ decreases by 0.2 permil/100 m increase in elevation [*Rose et al.*, 1996]. Uncertainty may be as large as several hundred meters (see text).

[c]Uncertainty is dominated by uncertainty in recharge elevation and is probably less than 1°C.

surface is negligible, the spring water is also discharging all the geothermal heat it acquires, and the spring temperature can be used to estimate the geothermal heat flux.

[17] We will assume that the small springs on the flanks of the volcano that discharge water at about 7°C [*Rose et al.*, 1996] are representative of the mean recharge temperature. The discharge temperature of the large-volume springs at lower elevations is about 12°C [*Mariner et al.*, 1998], and thus $\Delta T \approx 5$°C. We will further assume that the difference between the mean recharge elevation and discharge elevation (Δz in equation (4)) is about 1.5 km [*Rose et al.*, 1996], resulting in about 3°C of warming through GPE dissipation. Thus about 2°C of warming can finally be attributed to geothermal warming, equivalent to background heat flux $Q = \rho_w C_w /2000\ \mathrm{km}^2 \times 40\ \mathrm{m}^3\ \mathrm{s}^{-1} \times 2°\mathrm{C} \approx 0.16\ \mathrm{W/m}^2$. This background heat flux is similar to that elsewhere in the Cascades arc [e.g., *Blackwell et al.*, 1990]. If we had ignored the contribution of GPE dissipation in this calculation, we would have incorrectly obtained $Q \approx 0.46\ \mathrm{W/m}^2$ [*Manga*, 2001], much larger than anywhere else in the Cascades [*Blackwell et al.*, 1990].

5. Interpreting Spring Temperatures: Application to Cold Springs in the Oregon and California Cascades

[18] In the Oregon and California Cascades, high recharge rates combined with a poorly dissected landscape result in the formation of many large springs. The resulting rapid and voluminous groundwater flow causes an advective disturbance to the subsurface temperature gradient that makes the use of borehole temperature measurements to determine heat flow challenging and controversial [*Ingebritsen et al.*, 1996a, 1996b; *Blackwell and Priest*, 1996a, 1996b]. In this region, previous studies have shown that advectively transported heat discharged by hot springs represents a substantial fraction of the heat budget of the volcanic arc [*Ingebritsen et al.*, 1989].

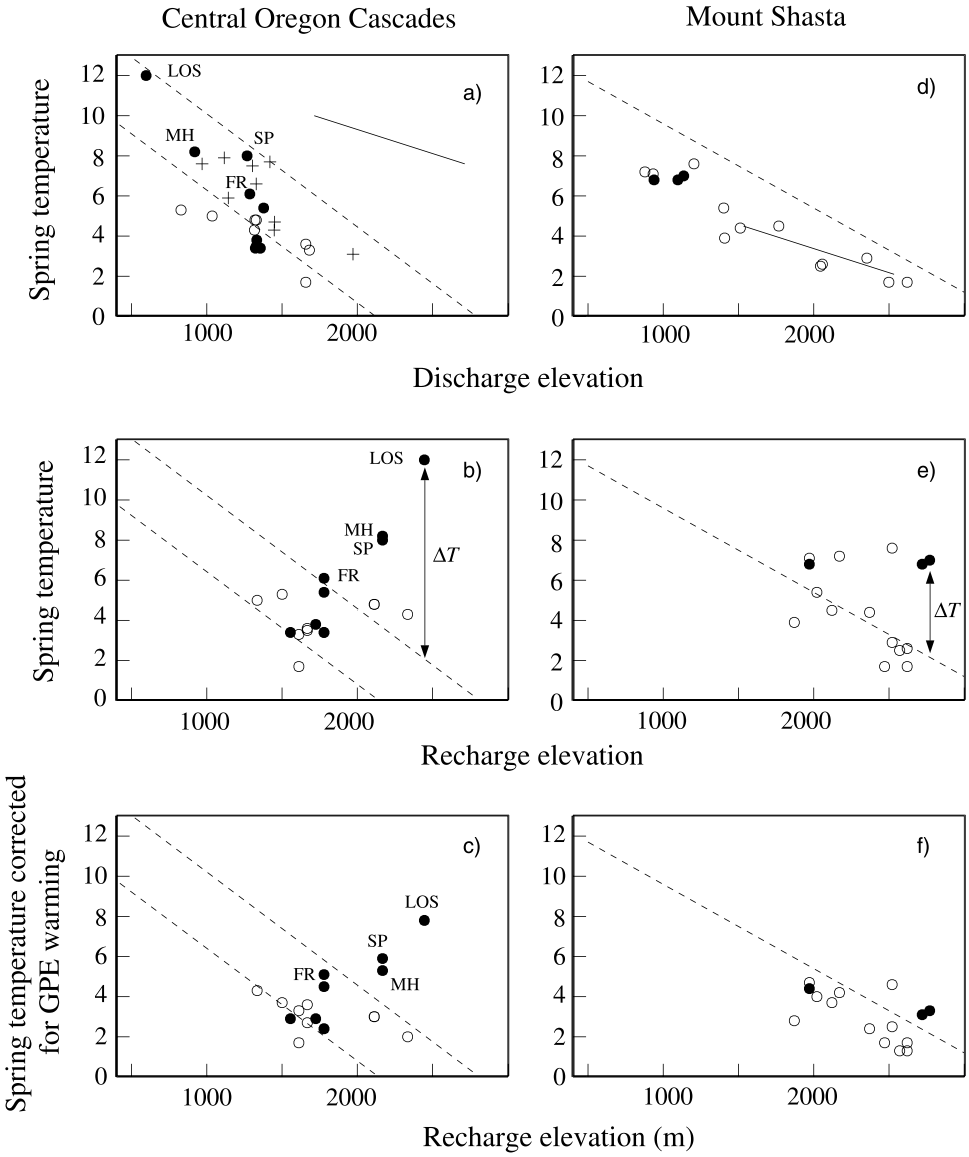

Figure 5. Relationship between elevation and spring water temperature in the central Oregon Cascades (left column of figures) and Mount Shasta, California (right column of figures). Data are compiled from *James* [1999] and *Nathenson et al.* [2003] and listed in Table 1. Solid circles indicate large-volume springs with mean discharges >0.5 m^3/s (Oregon) and >0.2 m^3/s (Mount Shasta). Open circles indicate smaller springs. The plus signs show the mean annual surface temperature at climate stations in the region (data from Oregon Climate Service). (a and d) Spring temperature as a function of discharge elevation. (b and e) Spring temperature as a function of the mean recharge elevation inferred from the oxygen isotope content of the spring water. The uncertainty in this inferred recharge elevation could be as much as 200 m (see text for details). The temperature difference ΔT shows the amount of warming of the water between the recharge elevation and discharge elevation. (c and f) Spring temperature at the recharge elevation corrected for the expected 2.3°C/km increase in water temperature as the water flows to lower elevations. The temperature difference ΔT now indicates the amount of geothermal warming of the water, assuming all geothermal heat added to the water is retained by the water. Solid lines in Figures 5a and 5d show the GPE dissipation lapse rate. The dashed curves show the relationship between elevation and surface temperature (Figures 5d–5f) or upper and lower bounds on the relationship between elevation and temperature (Figures 5a–5c). Oregon spring names (see map) are SP, Spring Creek; FR, Fall River; MH, Metolius Headwaters; and LOS, Lower Opal Springs.

[19] In the Cascades, large-volume cold springs, despite their low temperatures, might also be discharging large amounts of geothermal heat because of their large discharge [*Manga*, 1998]. In this section we reexamine the temperature of cold springs. In our analysis we will assume that heat conduction to and from the surface is negligible because aquifer depths are typically greater than many tens of meters [e.g., *Gannett et al.*, 2003], and

Figure 2b implies that ΔT should be dominated by GPE and geothermal warming.

[20] We consider a set of springs located east of the crest of the central Oregon Cascades (Figure 4) and a set of springs on the flanks of Mount Shasta in the California Cascades. Data for these two regions come from *James* [1999] and *Nathenson et al.* [2003], respectively, and are summarized in Table 1.

[21] Figures 5a and 5d show spring temperatures as a function of the discharge elevation in the Oregon Cascades and at Mount Shasta, respectively. The dashed line in Figure 5d (and Figures 5e and 5f as well) shows the relationship between the mean annual surface temperature and elevation inferred from climate stations near Mount Shasta [*Nathenson et al.*, 2003]. The slope of the dashed line is 4.5°C, consistent with a moist adiabatic lapse rate. The plus signs in Figure 5a show mean annual surface temperature as a function of elevation at climate stations in the Oregon Cascades, and we expect that the mean annual surface temperature should lie somewhere between the two dashed lines. The scatter of climate station temperatures in Oregon probably reflects local climate variations that are influenced by the various mountain chains in this region. By contrast, the linear relation between temperature and elevation found at Mount Shasta [*Nathenson et al.*, 2003] reflects minimal spatial climatic variations, as would be expected for temperature measurements from the slopes of a single volcano. Figures 5a and 5d show that most springs discharge water at temperatures similar to, or colder than, the mean annual surface temperature.

[22] The solid lines in Figures 5a and 5d show the GPE dissipation lapse rate. That is, if all the spring water has the same recharge elevation and recharge temperature, and there is no heat transfer with the surface or addition of geothermal heat, then spring temperature as a function of elevation should have the same slope as the solid line. The high elevation cold springs at Mount Shasta do in fact exhibit this slope.

[23] In Figures 5b and 5e we plot the spring temperature as a function of the recharge elevation. Figures 5b and 5e show that some of the springs discharge water that is several degrees warmer than the temperature at the recharge elevation. This temperature change, ΔT, is given by equation (4) in the special case that heat transfer to and from the surface can be neglected. The recharge elevation in Figure 5 is estimated by using the oxygen isotope composition of the spring water as a tracer of recharge elevation. In mountainous regions, precipitation becomes progressively more depleted in the heavier isotope of oxygen due to rainout as air masses change elevation. In the Oregon and California Cascades, the isotopic composition of precipitation decreases by about 0.2 permil/100 m rise in elevation [*Rose et al.*, 1996; *James et al.*, 2000]. For the springs in the Oregon Cascades, *James et al.* [2000] calculated the recharge elevation of spring water following this approach, and their inferred recharge elevations are shown in Figure 5b. Assuming there is a single relationship between $\delta^{18}O$ and elevation, and that the variation of the isotopic composition of snow core data is due to stochastic variability with time, the standard error in the inferred recharge elevation ranges from 75 m at an elevation of 1700 m to 235 m at the highest inferred recharge elevation. These isotopically inferred recharge elevations are also consistent with those obtained by *Manga* [1998] from mass-balance considerations. For the Mount Shasta springs, Figure 5e, we assume that the Green Butte springs discharge locally recharged water and that $\delta^{18}O$ also decreases by 0.2 permil/100 m rise in elevation. In both regions the spring water compositions fall on local meteoric water lines, implying that the isotopic composition of the water (and thus our inferred recharge elevation) is not significantly affected by evaporation. At Mount Shasta, the uncertainty in recharge elevation cannot be determined, but may be as large as 200 m. The uncertainty in ΔT due to an uncertainty in recharge elevation of 200 m is 1°C.

[24] Figures 5c and 5f show the temperature of the spring water, corrected for the expected GPE warming, as a function of the mean recharge elevation. In the limit that we can neglect heat transfer to and from the surface (again, a reasonable approximation in the Cascades because of high recharge, typically 0.5 m/yr), the increase in GPE-corrected temperature can be attributed to geothermal warming. At Mount Shasta (Figure 5f), there is scant evidence of geothermal warming. In the Oregon Cascades, several large springs show some geothermal warming, although a comparison of Figure 5b and Figure 5c shows that a large fraction of ΔT is caused by GPE dissipation. A GPE-corrected ΔT of 5°C for Lower Opal Springs (discharge 6.8 m^3/s) still implies a geothermal heat discharge of 140 MW, larger than that of any hot spring in the region [*Ingebritsen et al.*, 1994].

[25] Figures 5c and 5f also suggest that the mean recharge temperature may be between about 1 and 2 degrees cooler than the mean annual surface temperature at the recharge elevation, probably because recharge is dominated by snowmelt during the springtime. Although this is only a small deviation from the common approximation that the recharge temperature is the same as the mean annual surface temperature [e.g., *Taniguchi*, 1993], this temperature difference should be accounted for when interpreting the temperature of cold springs because it can be a large fraction of ΔT.

6. Conclusions

[26] At hot springs, the high temperature of the discharged water is clearly dominated by geothermal warming at depth. In contrast, interpreting the temperature of cold springs or "slightly thermal" springs [*Nathenson et al.*, 2003] is inherently challenging because the temperature change ΔT is small. Here we have shown that the conversion of gravitational potential energy to heat can be an important source of warming for many large-volume cold springs and must be accounted for when interpreting spring temperatures in mountainous regions. Correcting for the effects of GPE warming yields significantly lower estimates of the contribution of geothermal warming to spring temperatures in the Oregon and California Cascades.

[27] **Acknowledgments.** This work was supported by NASA Astrobiology Institute, agreement NNA04CC02A. The authors thank the anonymous A.E., H. Gonnermann, M. O. Saar, and two anonymous reviewers for useful comments and suggestions.

References

Andrews, J. N., W. C. Burgess, W. M. Edmunds, R. L. F. Kay, and D. J. Lee (1982), The thermal springs of Bath, *Nature*, *298*, 339–343.

Blackwell, D. D., and G. R. Priest (1996a), Heat flow from four new research drill holes in the western Cascades, Oregon, USA: Comment, *Geothermics*, *25*, 703–713.

Blackwell, D. D., and R. R. Priest (1996b), Comment on "Rates and patterns of groundwater flow in the Cascade Range volcanic arc and the effect on subsurface temperatures" by S. E. Ingebritsen, D. R. Sherrod, and R. H. Mariner, *J. Geophys. Res.*, *101*, 17,561–17,568.

Blackwell, D. D., J. L. Steele, S. Kelley, and M. A. Korosec (1990), Heat flow in the state of Washington and thermal conditions in the Cascade range, *J. Geophys. Res.*, *95*, 19,945–19,516.

Brott, C. A., D. D. Blackwell, and J. P. Ziagos (1981), Thermal and tectonic implications of heat flow in the eastern Snake River Plain, Idaho, *J. Geophys. Res.*, *86*, 11,709–11,734.

Bundschuh, J. (1993), Modeling annual variations of spring and groundwater temperatures associated with shallow aquifer systems, *J. Hydrol.*, *142*, 427–444.

Davis, S. N. (1999), Humboldt, Arago, and the temperature of groundwater, *Hydrogeol. J.*, *7*, 501–503.

Domenico, P. A. (1972), *Concepts and Models in Groundwater Hydrology*, 405 pp., McGraw-Hill, New York.

Fisher, A. T., and K. Becker (2000), Channelized fluid flow in oceanic crust reconciles heat-flow and permeability data, *Nature*, *403*, 71–74.

Forster, C., and L. Smith (1989), The influence of groundwater flow on thermal regimes in mountainous terrain: A model study, *J. Geophys. Res.*, *94*, 9439–9451.

Gannett, M. W., M. Manga, and K. E. Lite Jr. (2003), Groundwater hydrology of the upper Deschutes Basin and its influence on streamflow, in *A Peculiar River: Geology, Geomorphology, and Hydrology of the Deschutes River, Oregon*, *Water Sci. Appl. Ser.*, vol. 7, edited by J. E. O'Conner and G. E. Grant, pp. 31–50, AGU, Washington, D. C.

Ingebritsen, S. E., D. R. Sherrod, and R. H. Mariner (1989), Heat flow and hydrothermal circulation in Cascade range, north-central Oregon, *Science*, *243*, 1458–1462.

Ingebritsen, S. E., R. H. Mariner, and D. R. Sherrod (1994), Hydrothermal systems of the Cascade range, north-central Oregon, *U.S. Geol. Surv. Prof. Pap.*, *1044-L*, 86 pp.

Ingebritsen, S. E., M. A. Scholl, and D. R. Sherrod (1996a), Heat flow from four new research drill holes in the western Cascades, Oregon, USA: Reply, *Geothermics*, *25*, 715–724.

Ingebritsen, S. E., D. R. Sherrod, and R. H. Mariner (1996b), Reply to comment on "Rates and patterns of groundwater flow in the Cascade range volcanic arc and the effect on subsurface temperatures," *J. Geophys. Res.*, *101*, 17,569–17,576.

James, E. R. (1999), Isotope tracers and regional-scale groundwater flow: Application to the Oregon Cascades, M.S. thesis, 150 pp., Univ. of Oreg., Eugene.

James, E. R., M. Manga, and T. P. Rose (2000), The use of temperature and the isotopes of O, H, C, and noble gases to determine the pattern and spatial extent of groundwater flow, *J. Hydrol.*, *237*, 100–112.

Langseth, M. G., and B. G. Herman (1981), Heat transfer in the oceanic crust of the Brazil Basin, *J. Geophys. Res.*, *86*, 10,805–10,819.

Manga, M. (1997), A model for discharge in spring-dominated streams and implications for the transmissivity and recharge of quaternary volcanics in the Oregon Cascades, *Water Resour. Res.*, *33*, 1813–1822.

Manga, M. (1998), Advective heat transport by low-temperature discharge in the Oregon Cascades, *Geology*, *26*, 799–802.

Manga, M. (2001), Using springs to study groundwater flow and active geologic processes, *Annu. Rev. Earth Planet. Sci.*, *29*, 201–228.

Mariner, R. H., W. C. Evans, and M. Huebner (1998), Preliminary chemical and isotopic data for waters from springs and wells on and near Medicine Lake Volcano, Cascade Range, northern California, *U.S. Geol. Surv. Open File Rep.*, *98-2*, 27 pp.

Meinzer, O. E. (1927), Large springs in the United States, *U.S. Geol. Surv. Water Supply Pap.*, *557*, 94 pp.

Nathenson, M. L., J. M. Thompson, and L. D. White (2003), Slightly thermal springs and non-thermal springs at Mount Shasta, California: Chemistry and recharge elevations, *J. Volcanol. Geotherm. Res.*, *121*, 137–153.

Pollack, H. N., S. J. Hurter, and J. R. Johnson (1993), Heat loss from the Earth's interior: Analysis of the global data set, *Rev. Geophys.*, *31*, 267–280.

Rose, T. P., M. L. Davisson, and R. E. Criss (1996), Isotope hydrology of voluminous cold springs in fractured rock from an active volcanic region, northeastern California, *J. Hydrol.*, *179*, 207–236.

Rosenberg, N. D., A. T. Fisher, and J. S. Stein (2000), Large-scale heat and fluid transport in the seafloor: Revisiting the well-mized aquifer model, *Earth Planet. Sci. Lett.*, *182*, 93–101.

Taniguchi, M. (1993), Evaluation of vertical groundwater fluxes and thermal properties of aquifers based on transient temperature-depth profiles, *Water Resour. Res.*, *29*, 2021–2026.

van der Kamp, G., and S. Bachu (1989), Use of dimensional analysis in the study of thermal effects of various hydrogeological regimes, in *Hydrogeological Regimes and Their Subsurface Thermal Effects*, *Geophys. Monogr. Ser.*, vol. 47, edited by A. E. Beck, G. Garven, and L. Stegena, pp. 23–28, AGU, Washington, D. C.

J. W. Kirchner and M. Manga, Department of Earth and Planetary Science, University of California, Berkeley, 307 McCone Hall, Berkeley, CA 94720, USA. (manga@seismo.berkeley.edu)